Número Suplemento

Ingeniería y
Competitividad
Vol 25 (suplemento) 2023; doi: 10.25100/iyc.v25isuplemento13117

ISSN
0123-3033
e- 2027-8284

Artículo de investigación

Edición especial 25 años del doctorado en ingeniería

Dynamic simulation of a flotation column

Simulación dinámica de una columna de flotación

Cómo citar: Piñeres, J., Barraza, J., Grecco, A., Calvo, M.Dynamic simulation of a flotation column. Ingeniería y Competitividad. 25(suplemento) ,e- 20913117. doi: 10.25100/iyc.v25isuplemento.13117

Jorge Piñeres[1§], Anderson Grecco[1], Milene Calvo[1]

[1§]Grupo de Investigación en Simulación de Procesos y Transformación del Carbón Programa de Ingeniería Química, Universidad del Atlántico, Barranquilla, Colombia

jorgepineres@mail.uniatlantico.edu.co, andersongrecco@hotmail.com, milenecalvo_26@hotmail.com

Abstract

This paper describes the dynamic behavior in a flotation column from the development of a mathematical model of distributed parameters for the collection and the froth zone in order to select appropriate control strategies that will allow us to optimize the operation and improve its performance. For the solution of the mathematical model, the numerical method used was the finite element method. The proposed model includes sub-processes such as particle-bubble collection and detachment and bubble coalescence in the froth zone, among others. For the simulation, each zone of the flotation column is subdivided into volume elements, assuming each volume element is a perfectly mixed tank. The results show that the model adequately describes both the behavior of the collection zone and the froth zone, which are related to each other. During the validation of the mathematical model, satisfactory results were obtained when comparing the experimental data with those obtained through the simulation with low percentages of error (average error less than 5%).

Keywords: Column flotation, mathematical model, collection zone.

Resumen

En este trabajo se describe el comportamiento dinámico en una columna de flotación a partir del desarrollo de un modelo matemático de parámetros distribuidos para la zona de colección y la zona de espumante con el objeto de seleccionar estrategias de control apropiadas, que nos permitan optimizar la operación y el mejorar su desempeño. Para la solución del modelo se usó el método de los elementos finitos. El modelo propuesto incluye subprocesos tales como la colección y el desprendimiento partícula-burbuja, la coalescencia de burbujas en la región de espumante, entre otros. Para la simulación se subdivide cada zona de la columna de flotación en elementos de volumen, asumiendo cada elemento como un tanque de mezcla perfecta. Los resultados muestran que el modelo describe adecuadamente tanto el comportamiento de la zona de colección como la de espumante las cuales se encuentran relacionadas entre sí. Durante la validación del modelo se obtuvieron resultados satisfactorios al comparar los datos experimentales con los obtenidos a través de la simulación con bajos porcentajes de error (error promedio menor al 5%).

Palabras clave: Columna de flotación, modelo matemático, zona de colección.

doi: 10.25100/iyc.v25isuplemento.13117

Introduction

The use of flotation columns has extended in the mineral preparation plants due to the advantages it offers concerning the use of conventional flotation cells. Flotation is a physical-chemical separation process where a solid-solid separation is carried out where three phases interact (solid phase, liquid phase, and gas phase). This process allows the complex minerals benefit that present selectivity problem in a single cleaning stage. The column flotation substantially increases the concentration degree of the product desired and the mass yield of many minerals (1, 2).

Process control in the mineral processing industry is principally based on three components: measurement equipment specially designed for a particular system, the mathematical model for process analysis, and control strategies implemented through the make of computers (dynamic simulations). These components ensure control of process variables (3). A description of the flotation column dynamics would therefore be useful for experimenting with a diversity of automatic control process techniques that have been successfully applied in chemical engineering. The mathematical model proposed attempts to provide a good representation of the flotation column's dynamic behavior in both the collection and froth zones. However, to select a control strategy that adequately adjusts to the needs of a process, it is necessary to develop a mathematical model that allows an appropriate description of the dynamic behavior (dynamic simulation) (4) proposed a dynamic simulator for flotation columns based on the conservation principle. The mathematical model was based on the application of a population balance developed a dynamic simulation for flotation columns based on a macroscopic description of the behavior of the slurry and gas using the global material balance and specific empirical models(5). Bouchard et al., (2014) (6) presented a dynamic simulation of the flotation columns. The simulation focused on the water, solids, and air flow rates and their effect on the interface level of the slurry and the tailing flow rate. Yahui et al., (2018) (7) proposed a discrete dynamic model of three phases in flotation columns. The system is described by transporting nonlinear hyperbolic partial differential equations. The dynamics of the discrete model are compared with high-fidelity numerical simulations of the continuous linearized model to demonstrate the applicability of the proposed discrete model development. Yianatos et al., (2020) (8) developed a general flotation model based on industrial data and mechanical flotation cells, considering metallurgical performance, residence time distribution, and operating and hydrodynamic conditions.

In this paper, a mathematical model is proposed and provides a good representation of the dynamic behavior of a flotation column, including the factor that directly affects its performance, such as the collection, adhesion, particle-bubble detachment, coalescence of the bubbles in the froth zone, among others. This model adequately describes the behavior of the collection zone and the froth zone, which are related to each other through the interchange of material. This mathematical model describes the dynamic behavior of the gas and solid phases simultaneously throughout the entire column. Usually, the froth zone used to be considered as a black box characterized only by a recovery value (mass yield). The present model shows a reasonable description of the dynamics of the flotation column, which is very useful for experimenting with a variety of control techniques that have been successfully applied in chemical engineering.

Mathematical model

A model balance distributed parameters (transport phenomena) is proposed to evaluate for a flotation column dynamic behavior. This model is based on the conservation principle. The general form balance equation is (4, 9):

doi: 10.25100/iyc.v25i4.13117

$$\frac{\partial \Phi}{\partial t} + \frac{\partial v \Phi}{\partial z} + PD - PA = \frac{1}{V_Z}(Q_e \Phi_e - Q_s \Phi_s) \quad (1)$$

where: Φ represents the variable or species under consideration, the first term in Eq (1) represents the change of Φ with respect to time, the second term in Eq (1) refers to the axial variation of Φ, the third and fourth terms represent the generation of the species under consideration. The term on the right-hand side in Eq (1) represents the net flow rate of the species under consideration through the system volume. The finite element method (FEM) was used to solve the mathematical model equations, in this manner; a partial differential equation is converted into an ordinary differential equation (10). During the transformation, each zone of the flotation column is subdivided into volume elements, assuming each volume element has behavior as a perfectly mixed tank (perfectly mixed zones). The flotation column is a separation process; that operates with 3 phases (liquid-solid-gas). The column consists of two zones; the *collection zone*, where particle-bubble contact occurs, and the *froth zone*, where bubbles loaded with hydrophobic particles get. In the collection zone is where the feed flow rate enters the flotation column. It might be divided into a lower collection zone (from the aeration zone to the feeder point) and an upper collection zone (from the feeder point to the pulp-froth interface). The feeder point zone is taken as a transition zone. To provide simplicity to the mathematical model, it is necessary to make several assumptions. Table 1 shows the assumptions made during mathematical model development:

Table 1. Assumptions

Collection zone	Froth zone
1. Perfect mixing tank. 2. Aeration, feed, wash water and interface are transition zones. 3. Constant particle diameter. 4. Nc compositions, in this mathematical model Nc = 2, organic matter (desired) mineral matter (undesired). 5. Constant bubble diameter, there is no coalescence of the bubbles. 6. There is no detachment of particles. 7. The bubble is considered a rigid sphere and not mobile.	1. Spherical and rigid bubbles. 2. Piston flow 3. Constant froth depth. 4. Constant air hold-up. 5. Bubbles coalescence. 6. Detachment of particles. 7. There is no particles collection

Bubble diameter: the bubble diameter is calculated from (11 - 13):

$$D_{bub} = C J_g^{\,n} \quad (2)$$

where D_{bub} is the bubble diameter, *C* (corresponds to the mean bubble diameter at a superficial gas velocity of 1 cm/sec and is a function of frother concentration and bubble generator dimension) is a proportionality constant that changes according to the change of air flow rate and J_g is the superficial air velocity, *n* is a constant than varies between 0.2 and 0.3, for a range of J_g between 1 and 3 cm/sec (11 – 13).

Available load fraction of the bubble: the available load fraction of the bubble is calculated from (4, 13, and 14):

$$\beta l_c = \frac{Cmpa_c D_{bub}}{4 \rho_{p_c} d_p^{\,e}} \quad (3)$$

doi: 10.25100/iyc.v25isuplemento.13117

where $Cmpa_c$ is the attached particles mass concentration of composition c, ε is the air hold-up, d_p is the particle diameter and ρ_{p_c} is the particle density of composition c.

Slurry density: the authors proposed than the liquid-solid set composes the slurry, the slurry mass of the particles for a determined zone is defined as $Cmpl_c(1-\varepsilon)Vz$, the liquid mass in a given zone is given by $\rho_w(1-\varepsilon)Vz$ and the volume occupied by the slurry in a given zone is $(1-\varepsilon)Vz$, are defined as (15):

$$\rho_{sl} = \frac{\text{Mass of slurry}}{\text{Volume of slurry}} \tag{4}$$

$$\rho_{sl} = \frac{\text{Mass (solid+liquid)}}{\text{Volume of slurry}} \tag{5}$$

$$\rho_{sl} = \frac{\text{Mass (organic matter (C1) and mineral matter (C2)+water)}}{\text{Volume of slurry}} \tag{6}$$

$$\rho_{sl} = \frac{Cmpl_{\text{organic matter}}(1-\varepsilon)Vz + Cmpl_{\text{mineral matter}}(1-\varepsilon)Vz + \rho_w(1-\varepsilon)Vz}{(1-\varepsilon)Vz} \tag{7}$$

$$\rho_{sl} = Cmpl_{c1} + Cmpl_{c2} + \rho_w \tag{8}$$

$$\rho_{sl} = \sum_{c=1}^{Nc} Cmpl_c + \rho_w \tag{9}$$

where ρ_{sl} is the slurry density, $Cmpl_c$ is the free particles mass concentration of composition c, ρ_w is the water density, Vz is the volume of zone z.

Bubble density: the authors proposed than the hexagonal particle arrangement generates the largest possible amount of particles in the available area of the bubble, assuming that this arrangement occurs in the flotation process, the amount of attached particles is calculated according to the load fraction and the area fraction available as below (Figure 1).

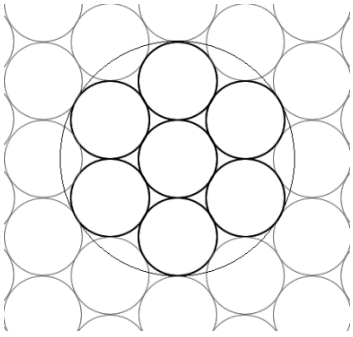

Figure 1. Fraction of area available to attach particles

Figure 1 shows seven circles inscribed in the inside part of a circle with a radius three times greater than the area fraction not occupied by the small circles was estimated, as $(9\pi r^2 - 7\pi r^2)/9\pi r^2$ giving an available fraction of $(1-2/9)$. $Npbub_c$ is calculated by multiplying the bubble area by the load fraction of the bubble for each component and the available area fraction; this is divided by the

doi: 10.25100/iyc.v25i4.13117

area of each particle resulting in the particle number of composition c on the bubble (15):

$$Npbub_c = \frac{\beta l_c \left(1-\frac{2}{9}\right) D_{bub}{}^2}{d_p{}^2} \quad (10)$$

where $Npbub_c$ is the particles number of composition c attached in a bubble, βl_c is the load fraction of the bubble for composition particles c. Knowing the particles number of composition c attached to each bubble, the mass-volume ratio of the particle-bubble set is calculated. The bubble density is calculated from the following expression (15):

$$\rho_{bub} = \frac{\text{Mass of bubble}}{\text{Volume of bubble}} \quad (11)$$

$$\rho_{bub} = \sum_{c=1}^{Nc} \rho_{bub_c} \quad (12)$$

$$\rho_{bub_c} = \frac{d_p{}^3 Npbub_c \rho_p + D_{bub}{}^3 \rho_{bub_i}}{d_p{}^3 Npbub_c + D_{bub}{}^3} \quad (13)$$

where ρ_{bubc} is the bubble density loaded with composition particles c, ρ_{bubi} is the initial bubbles density and ρ_{bub} is the bubble density that is defined as the sum of each of the densities for a specific particle composition.

Suspension density: the liquid-solid-gas (bubbles) set make up the suspension, the suspension density can be calculated from (13, 15):

$$\rho_{susp} = \varepsilon \rho_{bub} + (1-\varepsilon)\rho_{sl} \quad (14)$$

where ρ_{susp} is the suspension density.

Slurry viscosity: the slurry viscosity μ_{sl} was calculated using the relationship of (17):

$$\mu_{sl} = \mu_w \left(1 + 2.5fvp + 10.05fvp^2 + \ 0.00273e^{16.6fvp}\right) \quad (15)$$

where

$$fvp = \sum_1^{Nc} \left(\frac{Cmpl_c}{\rho p_c (1-\varepsilon)}\right) \quad (16)$$

μ_w is the water viscosity and fvp is the particles volumetric fraction present in the slurry

Slip and terminal velocity: the slip velocity Usg is the air velocity relative to the slurry (bubble swarms). The terminal velocity Ut is the ascent velocity of a single bubble (ε = 0). The bubbles velocities were calculated from (13, 16):

$$Ut = \frac{g D_{bub}{}^2 (\rho_{bub} - \rho_w)}{18\mu_w \left(1+0.15 Re_{bub}{}^{0.687}\right)} \quad (17)$$

$$Re_{bub} = \frac{D_{bub} Ut \rho_w}{\mu_w} \quad (18)$$

doi: 10.25100/iyc.v25isuplemento.13117

$$m = [4.45 + 18(D_{bub}/Dc)]Re_{bub}^{-0.1} \text{ if: } Re_{bub} < 200 \quad (19)$$

$$m = 4.45Re_{bub}^{-0.1} \text{ if: } Re_{bub} > 500 \quad (20)$$

$$m = 2.39 \text{ if: } 200 < Re_{bub} < 500 \quad (21)$$

$$Usg = \frac{gD_{bub}^{2}(\rho_{bub}-\rho_{sl})(1-\varepsilon)^{m-2}}{18\mu_{sl}(1+0.15Res^{0.687})} \quad (22)$$

$$Res = \frac{D_{bub}Usg\rho_{sl}(1-\varepsilon)}{\mu_{sl}} \quad (23)$$

where g acceleration due to gravity, Re_{bub} is the Reynolds number for a single bubble, Res is the Reynolds number for a bubble swarm, Dc is the flotation column diameter y *m* is a dimensionless parameter.

Settling and terminal velocity of particles: the terminal velocity of the particles is given by (18):

$$Ut_p = \frac{gd_p^{2}(\rho_p-\rho_w)}{18\mu_w(1+0.15Re_p^{0.687})} \quad (24)$$

$$Re_p = \frac{d_p Ut_p \rho_w}{\mu_w} \quad (25)$$

While the settling velocity of the particles is given

$$Ups = \frac{gd_p^{2}(\rho_p-\rho_{sl})(1-fvp)^{2.7}}{18\mu_w(1+0.15Reps^{0.687})} \quad (26)$$

$$Reps = \frac{dpUps\,\rho_w(1-fvp)}{\mu_w} \quad (27)$$

where Ut_p is the particle terminal velocity, Re_p is the Reynolds number for a single particle, Ups is the settling velocity for the whole set of particles and Reps is the Reynolds number for the set of particles.

Flotation rate equation: the flotation rate can be obtained from (13):

$$Cvf_c = \frac{1.5J_gP}{D_{bub}} \quad (28)$$

where Cvf_c is the rate constant of flotation for a particle of composition c, P is the probability of collection.

Collection zone: the following expression represents the total continuity equation in the stationary state of the flotation column:

doi: 10.25100/iyc.v25i4.13117

$$Qsl + Qpc = Qw + Qf \quad (29)$$

$$Qpc = Qw - Qb \quad (30)$$

where Qsl is the tailing flow rate, Qpc is the concentrate product flow rate, Qw is the wash water flow rate, Qf is the feed flow rate, Qb is the bias flow rate.

Air phase:

$$\frac{d\varepsilon}{dt} = \frac{Q_{in}\varepsilon_{in} - Q_{out}\varepsilon}{Vz} \quad (31)$$

The terms Q_{in} and Q_{out} represent enter and out flow rate (13):

In:
$$Q_{in}\varepsilon_{in} = (Qg - Qsl - A_c Ugs^{z-1}\varepsilon^{z-1})\varepsilon^{z-1} + A_c Ugs^{z-1}\varepsilon^{z-1} \quad (32)$$

Out:
$$Q_{out}\varepsilon = (Qg - Qsl - A_c Ugs^{z}\varepsilon^{z})\varepsilon^{z} + A_c Ugs^{z}\varepsilon^{z} \quad (33)$$

Qg, and A_C represent air flow rate and the column cross-sectional area respectively.

Free particles: the total continuity equation for the free particles of equal size but different composition in a perfectly mixed zone is expressed as:

$$\frac{\partial Cmpl_c}{\partial t} - PD_c + PA_c = \frac{1}{V_z}(Q_{in}\, Cmpl_c^{\,in} - Q_{out} Cmpl_c) \quad (34)$$

The PDc term is known as the particle detachment term and is equal to zero due to the assumption that particle detachment occurs in the collection zone. On the other hand, the PAc term, also known as the particle adhesion term, is calculated through the following expression (15):

$$PA_c = Cvf_c Cmpl_c \left(\frac{1-\beta l_c}{\beta_{max}}\right) \quad (35)$$

where $Cvf_{c,}$ is the particles flotation rate constant of equal size but different composition which collides with bubbles, the parameters βl_c y β_{max} represent the surface covered fraction by composition particles c in bubbles of known diameter and the maximum possible fraction of covered area, which in this case has been designated as 0.5, respectively (19):

In:
$$Q_{in}{}^{z} = A_c Ugs^{z+1} + A_c Ups_c{}^{z+1} + \left(Qg - Qsl + A_c Ugs^{z-1}(1-\varepsilon^{z-1})\right) \quad (36)$$

Out:
$$Q_{out}{}^{z} = A_c Ugs^{z} + A_c Ups_c{}^{z} + \left(Qg - Qsl + A_c Ugs^{z}(1-\varepsilon^{z})\right) \quad (37)$$

Attached particles: the attached particles are classified according to their size and composition

doi: 10.25100/iyc.v25isuplemento.13117

(floatability) and bubble size. However, in this work, it is assumed to be constant the bubble diameter (through the collection zone) and particle size. The total continuity equation (there is no particles detachment through the collection zone) is:

$$\frac{\partial \mathrm{Cmpa_c}}{\partial t} = \frac{(Q_{in}\,\mathrm{Cmpa_c^{in}} - Q_{out}\mathrm{Cmpa_c})}{\mathrm{Vz}} + \mathrm{Cvf_c Cmpl_c}\left(\frac{1-\beta \mathrm{l_c}}{\beta_{max}}\right) \quad (38)$$

In:

$$Q_{in}\mathrm{Cmpa_c^{in}} = (\mathrm{Qg} - \mathrm{Qsl^{z-1}} - \mathrm{A_c Ugs^{z-1}}\varepsilon^{z-1})\mathrm{Cmpa_c^{z-1}} + \mathrm{A_c Ugs^{z-1}Cmpa_c^{z-1}} \quad (39)$$

Out:

$$Q_{out}\mathrm{Cmpa_c} = (\mathrm{Qg} - \mathrm{Qsl^{z}} - \mathrm{A_c Ugs^{z}}\varepsilon^{z})\mathrm{Cmpa_c^{z}} + \mathrm{A_c Ugs^{z}Cmpa_c^{z}} \quad (40)$$

The term Qsl is defined according to the zone where the balance is carried out, located under the feeder point, this flow rate corresponds to the tailing flow rate, and above this corresponds to the bias flow rate.

Froth zone: the froth zone has a very complex behavior due to sub-processes such as bubble coalescence and particle detachment, among others. For the above reason the mathematical model proposed for this zone focuses on the assumptions exposed in Table 1.

Interface

Attached particles: the attached particle concentration at the interface is assumed to be the same as in the highest section of the collection zone, is considered that similar conditions such as bubble size and flow rate are maintained.

$$\mathrm{Cmpa_c^z} = \mathrm{Cmpa_c^{z-1}}\frac{\varepsilon^z}{\varepsilon^{z-1}} \quad (41)$$

Free particles: the total continuity equation for free particles of each species is represented as:

$$\frac{\partial \mathrm{Cmpl_c}}{\partial t} + \frac{(\mathrm{U_{pl}Cmpl_c})}{\partial z} + \mathrm{PA_c} - \mathrm{PD_c} = 0 \quad (42)$$

where PAc and PDc are equal to zero. U_{pl} represents the interstitial velocity for free particles, which given by the following relation (4, 20, and 21):

$$\mathrm{U_{pl}} = \frac{\mathrm{Q_{sl}}}{1-\varepsilon} + \mathrm{Ups} \quad (43)$$

where Ups is the particle settling velocity, the first term on the right hand-side of equation (43) represents the liquid net flow rate, resulting from the algebraic sum of the two types of flow rate, entrainment caused by bubble rise velocity and the drainage of the slurry through the wet film between bubbles. The drainage velocity Uds in a countercurrent system is defined as (4, 20, and 21):

$$\mathrm{Uds} = -\mathrm{Ugs} \quad (44)$$

The particle drag can be assumed to be directly proportional to the water drag and, the latter is

doi: 10.25100/iyc.v25i4.13117

considered the result of the average velocity rise bubbles. Therefore, for a countercurrent process, the net interstitial suspension flowing downward is given by the difference between the hindered average bubble rise velocity with respect to the slurry Ugs and the average velocity rise with respect to a stationary reference (4, 6, 20, and 21):

$$\frac{Qsl}{1-\varepsilon} = Ugs - \frac{Qg}{\varepsilon} \tag{45}$$

Substituting the corresponding terms, we have the following equation to describe the changes in the free particle´s concentration at the interface.

$$\frac{\partial Cmpl_c}{\partial t} + \frac{Q_{sl}}{1-\varepsilon} Cmpl_c{}^{z} - \frac{Q_{sl}}{1-\varepsilon} Cmpl_c{}^{z-1} + Ups_c\ Cmpl_c{}^{z+1} - Ups_c\ Cmpl_c{}^{z} = 0 \tag{46}$$

Stabilized froth zone

Attached particles: the total continuity equation for the change in the attached particles concentration in the stabilized froth zone is defined as:

$$\frac{\partial Cmpa_c}{\partial t} + \frac{v_{bub}\ Cmpa_c}{\partial z} + PD_c - PA_c = 0 \tag{47}$$

The particle adhesion term PAc is assumed to be zero in the froth zone, and the detachment term PDc is determined through the calculation based on the assumption that the reduction in the bubble's available surface area is due to the coalescence, given by the following equation (22):

$$PD_c = \frac{4DVzBl_c\rho_{p_c}d_p{}^{3}}{D_{bub}{}^{3}}\left(1 - \frac{2}{9}\right) \tag{48}$$

$$D = Recee(\varepsilon) \tag{49}$$

where D is considered the decrease in the bubble volumetric fraction of diameter Dbub as a consequence of coalescence, these terms consider the probability of the bubble's disappearance of size Dbub. The value (1 - 2/9) represents the usable bubble percentage. The *Recee* parameter is the coalescence efficiency ratio that corresponds to pairs of bubbles that interact in the stabilized froth zone. For this work, the authors assumed that the bubbles present the same diameter (4, 13). In this work, it is considered that the particle's detachment on the bubble surface occurs because of coalescence (reduction of specific bubble surface area), therefore; the particles that were attached to the bubble surface try to rearrange in the new bubble (big bubble) and, those that fail to do so due to the reduction in bubble surface area become detached. The average bubbles velocity v_{bub} is given by (15):

$$v_{bub} = \frac{J_g}{\varepsilon} \tag{50}$$

Substitute the terms into equation (48) to obtain:

$$\frac{\partial Cmpa_c}{\partial t} + \frac{J_g}{\varepsilon}\frac{\partial Cmpa_c}{\partial z} - Cmpa_c\frac{J_g}{(\varepsilon)^2}\frac{\partial \varepsilon}{\partial z} + \frac{4DVzBl_c\rho_{p_c}d_p{}^{3}}{D_{bub}{}^{3}}\left(1 - \frac{2}{9}\right) = 0 \tag{51}$$

doi: 10.25100/iyc.v25isuplemento.13117

Free particles: the equation corresponding to the change in the free particles concentration in the stabilized froth zone is similar to the equation proposed for the interface zone, with the difference that in this zone it is necessary to consider the term of particle detachment; to be represented from the following expression:

$$\frac{\partial Cmpl_c}{\partial t} + \frac{Qsl}{1-\varepsilon} Cmpl_c{}^{z} - \frac{Qsl}{1-\varepsilon} Cmpl_c{}^{z-1} + Ups_c\ Cmpl_c{}^{z+1} - Ups_c\ Cmpl_c{}^{z} - \frac{4DVzBl_c\rho_{p_c}d_p{}^{3}}{D_{bub}{}^{3}}\left(1-\frac{2}{9}\right) = 0 \quad (52)$$

Wash-water zone and draining froth: the addition of the wash water flow rate Qw at the column top increases the selectivity of the desired product, which indicates; its importance in flotation columns. When the wash-water flow rate enters, it separates into two currents with opposite directions, the downward current is called the bias flow rate Qb, and the upward one is the water flow rate that comes out together with the material desired by the top, the calculation of the bias flow rate is required throughout the simulation and was calculated from the following expression (13):

$$Qpc = \frac{Qg(1-\varepsilon_{top})}{\varepsilon_{top}} \quad (53)$$

$$Qb = Qw - Qpc \quad (54)$$

where ε_{top} is the air hold-up in the column top. The equations for free and attached particles established for the stabilized froth zone apply to both the wash-water zone and the draining froth zone because the system conditions are similar.

Attached particles:

$$\frac{\partial Cmpa_c}{\partial t} + \frac{J_g}{\varepsilon}\frac{\partial Cmpa_c}{\partial z} - Cmpa_c\frac{J_g}{(\varepsilon)^2}\frac{\partial \varepsilon}{\partial z} + \frac{4DVzBl_c\rho_{p_c}d_p{}^{3}}{D_{bub}{}^{3}}\left(1-\frac{2}{9}\right) = 0 \quad (55)$$

where D it is defined depending on the zone, for the wash-water zone (15):

$$D = Recal(\varepsilon) \quad (56)$$

For draining froth zone:

$$D = Recde(\varepsilon) \quad (57)$$

where $Recal$ and $Recde$ correspond to the efficiency ratio of coalescence of wash-water and draining froth respectively (4, 13):

Free particles

$$\frac{\partial Cmpl_c}{\partial t} + \frac{Qsl}{1-\varepsilon} Cmpl_c{}^{z} - \frac{Qsl}{1-\varepsilon} Cmpl_c{}^{z-1} + Ups_c\ Cmpl_c{}^{z+1} - Ups_c\ Cmpl_c{}^{z} - \frac{4DVzBl_c\rho_{p_c}d_p{}^{3}}{D_{bub}{}^{3}}\left(1-\frac{2}{9}\right) = 0 \quad (58)$$

doi: 10.25100/iyc.v25i4.13117

Recovery calculations: the overall flotation column recovery $RecColumn_c$ is (13):

$$RecColumn_c = \frac{RecFroth_c RecCollection_c}{1 - RecCollection_c + RecFroth_c RecCollection_c} \quad (59)$$

where $RecFroth_c$ it is the froth zone recovery with respect to the inputs coming from the collection zone and $RecCollection_c$ it is the collection zone recovery.

Collection zone recovery: to calculate recovery in the collection zone material balances in the upper collection zone must be carried out; due to the out stream from this zone being those that feed the interface zone and thus the froth zone. For calculations, we use the following expressions:

$$Entrained1_c = \left(Qg - Qb - A_c Ugs^z (1 - \varepsilon^z)\right) Cmpl_c^z \quad (60)$$

$$Floated1_c = (Qg - Qb - A_c Ugs^z \varepsilon^z) Cmpa_c^z + A_c Ugs^z Cmpa_c^z \quad (61)$$

$$Settling1_c = A_c Ugs^z Cmpl_c^{z+1} + A_c Ups_c^{z+1} Cmpl_c^{z+1} \quad (62)$$

$$RecCollection_c = \frac{Entrained1_c + Floated1_c}{Qfc_{f_c} + Sedimentado1_c} \quad (63)$$

where C_{fc} is the fed particles mass concentration of composition c. Equation (60) refers to the free particles that are entrained for the action of the air flow rate, passing from the upper collection zone to the froth zone. The terms of equation (61) represent the attached particle streams of composition c that were collected, in the collection zone and that crossed to the froth zone. Finally, the terms of equation (62) represent the free particles flow rate that comes from the froth zone and go back to the collection zone, either by the cleaning action of the bias flow rate or by the detachment of particles from the surface of the bubbles caused by the coalescence.

Froth zone recovery: froth zone recovery was calculated using a relationship is established between enter and out flow rates of this zone, considering the enter flow rates streams as those coming from the upper collection zone and the out flow rates as those coming from the drainage zone of the froth; calculated from the following expression proposed for the authors (15):

$$RecFrother_c = \frac{Entrained2_c + Floated2_c}{Entrained1_c + Floated1_c} \quad (64)$$

$$Entrained2_c = \frac{Qg\, Cmpl_c^z}{\varepsilon^z} \quad (65)$$

$$Floated2_c = \frac{Qg Cmpa_c^z}{\varepsilon^z} \quad (66)$$

Equations (65) and (66) represent the out flow rate through the top of the flotation column of free and attached particles, respectively. The flow rates along the flotation column are shown in Figure 2.

doi: 10.25100/iyc.v25isuplemento.13117

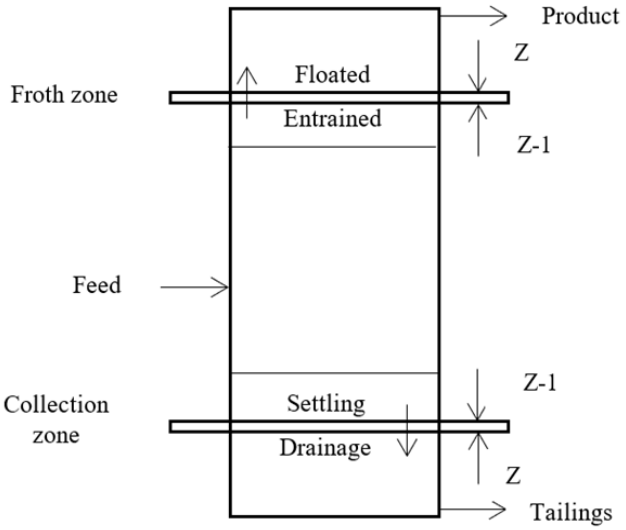

Figure 2. Flotation column zones

Results and Discussion

Simulations 1, 2, and 3: for the simulations and their code (based on Matlab), each zone of the flotation column was divided into sections to observe the axial mixing, to verify the model´s validity a simulation series were carried out with experimental results and literature-reported data. For the first and second simulations, experimental data were taken for two Colombian bituminous coals Cerrejon and Guachinte (1) while for the third simulation experimental data were taken for an Illinois bituminous coal (23). The number of sections into which each of the zones of the flotation column is divided, can be chosen. However, the higher the number of divisions, the more accurate the proposed mathematical model will have. During the simulations, two feed material components were defined for each coal sample; organic matter (component 1) and mineral matter (component 2). An adhesion probability of 0.4 for Cerrejon coal, 0.3 for Guachinte coal, and 0.5 for Illinois coal was established, while for mineral matter it was established as 0.05 (24). For the simulations with the Cerrejon and Guachinte coals a Jg of 0.7 cm/s was used, while for Illinois coal a Jg of 1.25 cm/s was used. Table 2 shows the operating conditions and parameters to perform simulations 1, 2, and 3 respectively.

doi: 10.25100/iyc.v25i4.13117

Table 2. Operating conditions and parameters for simulation 1, 2 and 3.

Characteristic of feed			
Coal sample	Cerrejon	Guachinte	Illinois
Coal density (gr/cm^3)	1.23	1.42	1.25
Mineral matter density (gr/cm^3)	2.55	2.55	2.55
Feed density SGf (gr/cm^3)	1.0047	1.0073	1.09
Particle diameter dp (cm)	0.0038	0.0038	0.0034
Percent solids Cs (w/w)	2.5	2.5	10.0
Solid distribution in the feed $Dcsf_c$	(0.8-0.2)	(0.65-0.35)	(50-50)
Ash percentaje (w/w) (db)	18.53	31.37	12.04
Superficial velocity (cm/s)			
Gas (air) superficial velocity (Jg)	0.7	0.7	1.25
Wash water superficial velocity (Jw)	0.3	0.3	0.31
Feed superficial velocity (Jf)	2.4	2.4	0.17
Characteristic of flotation column (cm)			
Diameter (dc)	5.5	5.5	5.0
Length of column (L)	500	500	170
Length of collection zone (Lc)	320	320	120
Length of froth zone (Lf)	120	120	50
Length of above the wash water point (Lw)	15	15	25
Length between interface and the feed point (Lif)	23	23	10
Length of transition zone (Lt)	2	2	2

Figure 3 shows the dynamic behavior of attached particles concentration in the different zones of the flotation column for the organic matter (component 1), Figure 4 shows the dynamic behavior of attached particles concentration for the matter mineral (component 2) from the Cerrejon, Guachinte and Illinois coals respectively. In these figures show an increasing trend of attached particles concentration as a function of time in the different zones of the flotation column, reaching steady-state in approximately 238, 190 and 112 seconds for component 1 and for component 2 to the 221, 137 and 84 seconds in the collection zone; at the interface and the froth zone, the curves are superimposed for the three coal samples, reaching the steady-state values for component 1 to the 337, 290 and 129 seconds and for component 2 to the 271, 179 and 154 seconds, finally at the top flotation column zone steady-state was reached approximately to the 415, 420 and 145 seconds for component 1 and for component 2 to the 393, 342 and 138 seconds for the three coal samples: Cerrejon, Guachinte and Illinois respectively.

doi: 10.25100/iyc.v25isuplemento.13117

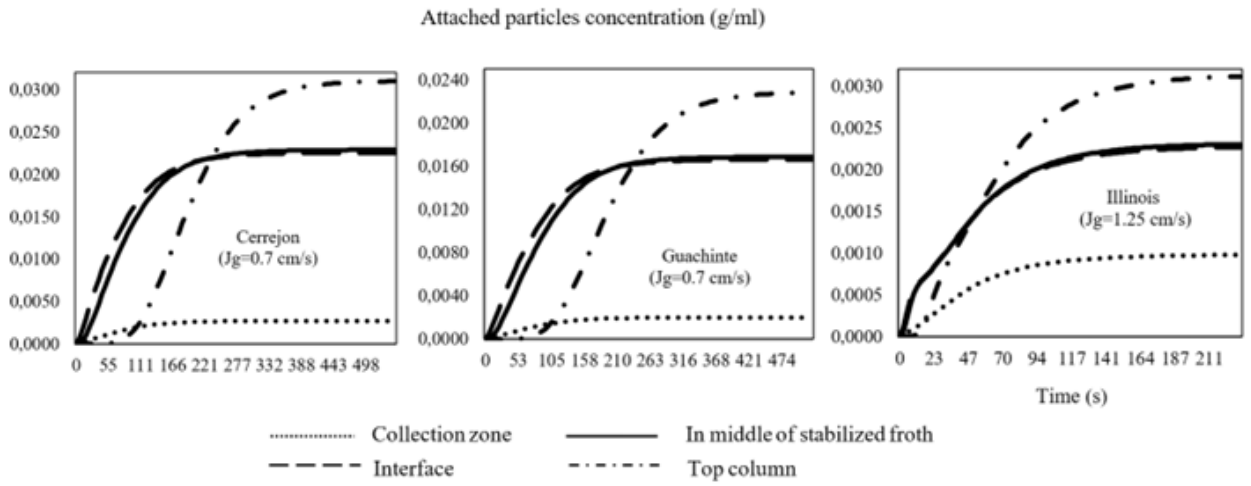

Figure 3. Dynamic in the concentration of attached particles in several zone of the column flotation for the organic matter (component 1).

The maximum concentration value of attached particles at the flotation column top for component 1 in the coal samples were 0.031 gr/ml for Cerrejon, 0.023 gr/ml for Guachinte and 0.0032 gr/ml for Illinois, while in the collection zone for Cerrejon, Guachinte and Illinois coals, the maximum values were 0.0027, 0.002 and 0.001 gr/ml respectively, with respect to interface and froth zone the curves are superimposed for the three coal samples, showing an approximate value for Cerrejon and Guachinte coals of 0.023 and 0.017 gr/ml respectively, while for Illinois coal of 0.0022 gr/ml.

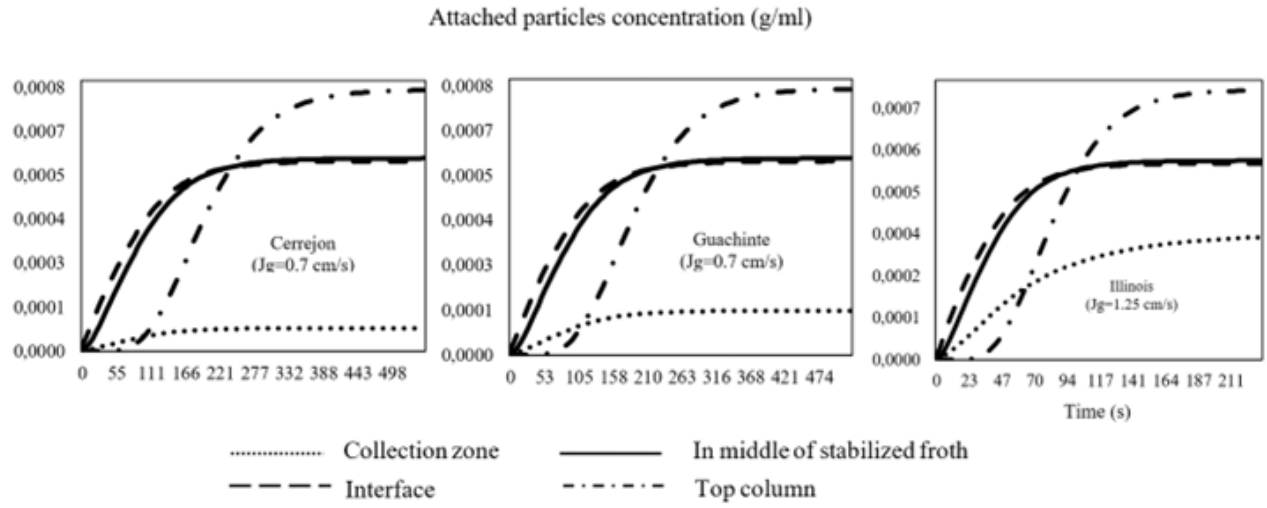

Figure 4. Dynamic in the concentration of attached particles in several zone of the column flotation for the mineral matter (component 2).

doi: 10.25100/iyc.v25isuplemento.13117

The maximum concentration value of component 2 as a time function for the three coal samples is approximately 0.0008 g/ml at the flotation column top, at interface and froth zone the curves are superimposed for component 2 for the three coal samples, showing approximately values of 0.00057 gr/ml, for the collection zone significantly different values are observed; $6.83x10^{-5}$ gr/ml for Cerrejon coal, 0.00013 gr/ml for Guachinte coal and 0.00035 gr/ml for Illinois coal, the values obtained for component 2 are considerably lower than those obtained for component 1 for the three coal samples, which may be attributed to a lower collection probability and a higher density, for what is expected this to obtained (component 2) in tailing flow rate the flotation column (1, 24). Figures 5 show the dynamic changes in the concentration of free particles in different areas of the flotation column for organic matter (component 1), and Figure 6 shows the dynamic changes in the free particle concentration for the mineral matter (component 2) of the Cerrejon, Guachinte, and Illinois coals respectively.

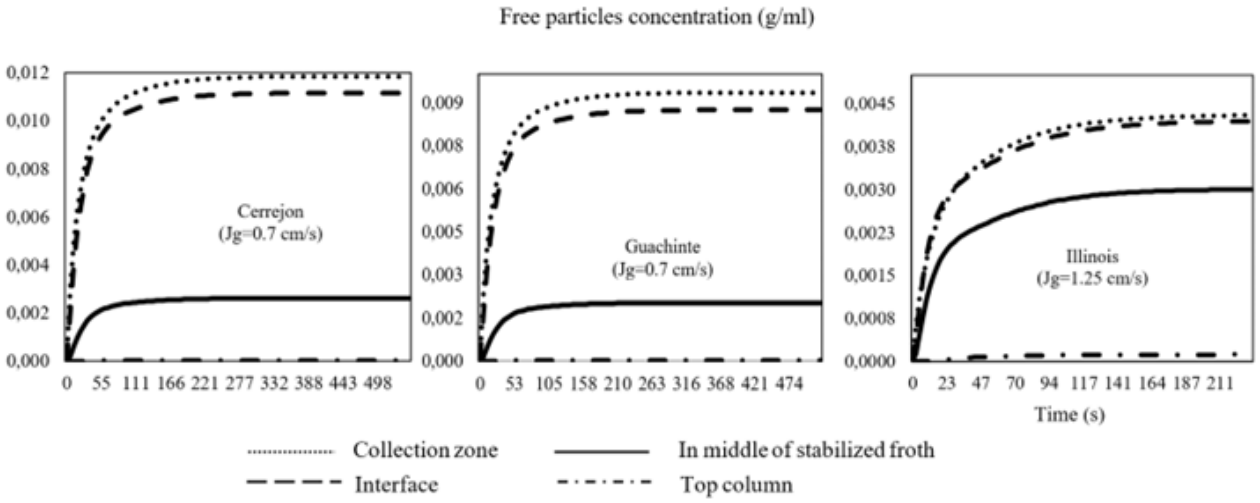

Figure 5. Dynamic in the concentration of free particles in several zone of the column flotation for the organic matter (component 1).

The profiles are shown in Figures 5 and 6 show that the free particle concentration (component 1 and component 2) decreases as one ascends along the different zones of the flotation column, reaching stability at approximately 227, 194, and 119 seconds for component 1 and for component 2 at 205, 168 and 145 seconds in the collection zone, 188, 194 and 100 seconds for component 1 and 150, 194 and 121 seconds for component 2 in the interface, for the froth zone there are values of 177, 142 and 75 seconds for component 1 and 138, 142 and 96 seconds for component 2, finally at the top of the flotation column stability was reached at approximately 210, 268 and 82 seconds for component 1 and for component 2 at 293, 273 and 160 seconds for the three coal samples: Cerrejon, Guachinte, and Illinois respectively.

doi: 10.25100/iyc.v25isuplemento.13117

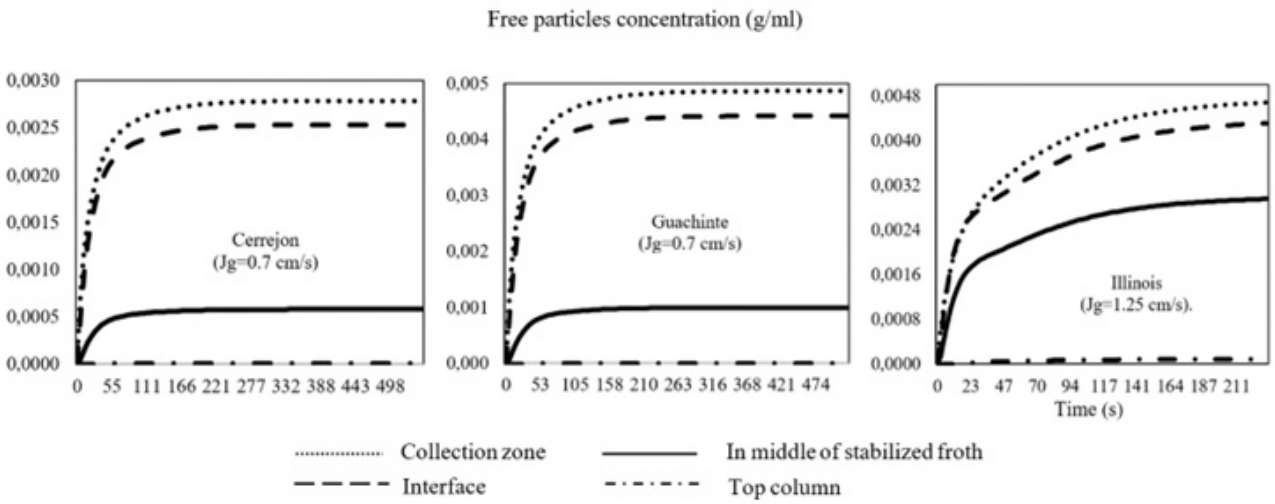

Figure 6. Dynamic in the concentration of free particles in several zone of the column flotation for the mineral matter (component 2).

It is observed in all the figures (Figure 3 and 4), that at the flotation column the mass concentration of free particles tends to zero, for component 1 values of $2.52x10^{-6}$, $1.83x10^{-6}$ and 0.0001 gr/ml were obtained for the Cerrejon, Guachinte and Illinois coals respectively, while for component 2 the values were $6.4x10^{-8}$ gr/ml for Cerrejon coal, $1.19x10^{-7}$ gr/ml for Guachinte coal and $8.96x10^{-5}$ for Illinois coal, while in the collection zone for the Cerrejon, Guachinte and Illinois coals, the maximum values were 0.012, 0.0094 and 0.0043 gr/ml of component 1 and 0.0028, 0.0049 and 0.0047 gr/ml of component 2, with respect to the interface for the three coal samples, the following values were obtained for component 1: 0.011, 0.0088 and 0.0042 gr/ml and for component 2: 0.0025, 0.0044 and 0.0043 gr/ml, finally for the froth zone the values for component 1 obtained are; 0.0026, 0.002 and 0.003 gr/ml, while for component 2 they are: 0.0006, 0.001 and 0.003 gr/ml respectively, showing the effectiveness of the froth zone, as a consequence of the presence of the washing water flow rate (bias flow rate). The presence of free particles of component 1 and component 2 of the coal at the top of the column flotation may be due to the entrainment of particles or to the detachment of the particles on the surface of the bubbles due to the coalescence phenomenon (25). In the same way, the presence of free particles of component 1 and component 2 in the froth zone can be explained through the entrainment of particles by the action of the incoming air flow rate; nevertheless, this concentration is considered negligible, indicating that the proposed mathematical model shows a good representation of the behavior of free and attached particles for component 1 and 2 in the flotation process.

Figures 7 show the profile of the air fraction along the flotation column. In these figures it can be seen that for the collection zone the air holdup is considerably lower compared to the froth zone, where an upward behavior is observed. The air fraction for the Illinois coal sample (0.29 in the collection zone) is higher than for Cerrejon and Guachinte coals (0.12 in the collection zone) due to their higher air velocity value. The increase of air holdup in the froth zone may be due to the absence of the slurry downdraft that allows air to predominate in this zone of the flotation column. For the Cerrejon and Guachinte coals, there is a slight decrease in the volumetric air holdup (0.08) at 300 cm length, while for the Illinois coal sample, this slight decrease (0.28) is observed at 120 cm, just at the feed point at the flotation column. Subsequently, the air holdup increases drastically

doi: 10.25100/iyc.v25isuplemento.13117

until approximately 0.64 at 320 cm for the Cerrejon and Guachinte coals and 136 cm for the Illinois coal, lengths that coincide with the interface of the flotation column, where the froth zone begins. The differences in the values of the air holdup in the collection zone compared to the values in the froth zone may due attributed to the low bubble ascent velocities due to the bubbles being loaded with particles on their surface (16). These results could indicate that the proposed mathematical model shows a good approximation of the hydrodynamic behavior of the flotation column.

Figures 8 show the mass concentration profile of attached particles concerning the height of the flotation column. It is observed in Figure 8 the maximum concentration reached by components 1 and 2 at the top of the flotation column; for Cerrejon coal, the maximum concentration particles attached 0.031 gr/ml for component 1 and 0.0008 gr/ml for component 2 was obtained at 445 cm of length, while for Guachinte coal the maximum concentration for component 1 was of 0.021 gr/ml and for component 2 of 0.0014 gr/ml, obtained at 445 and 437 cm of length, while for the Illinois coal, the maximum values of component 1 and 2 were obtained; 0.0031 gr/ml and 0.0011 gr/ml respectively at 174 cm length of the flotation column.

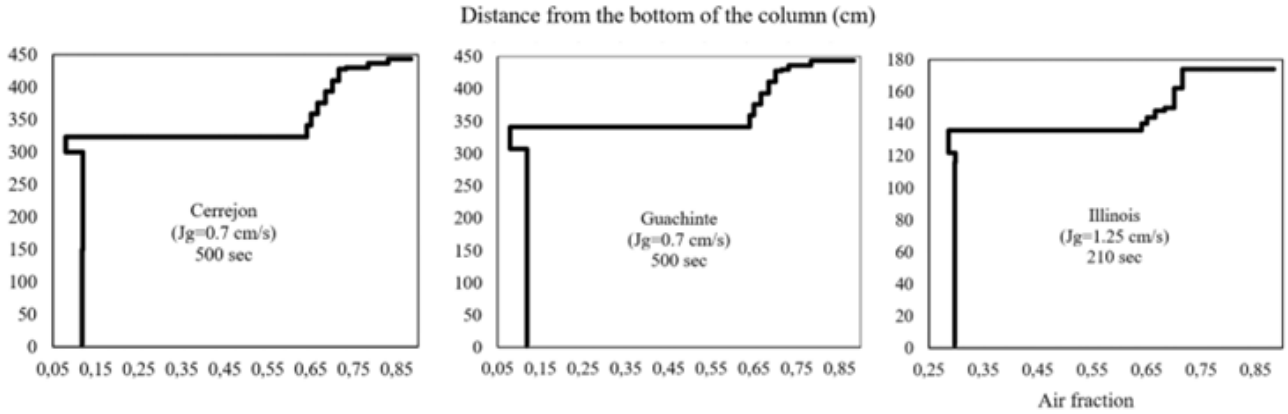

Figure 7. Air fraction profile along the column flotation

Organic matter (component 1) presents a concentration profile above this of mineral material (component 2). Significant increases in the concentration of component 1 are observed in the interface at 323 cm in length of the flotation column; for Cerrejon coal, it increases from 0.0028 to 0.02 gr/ml, and for Guachinte coal, the increase goes from 0.002 at 0.017 gr/ml, the interface for Illinois coal is located at 122 cm length of the flotation column and, presents an increase of component 1 from 0.0010 to 0.0023 gr/ml, this result may be related to the coal hydrophobicity. The line representing component 2 varies in a narrow concentration range. The accumulation of this component is not desired in the flotation process. The concentration values of this component compared that the desire component is low.

doi: 10.25100/iyc.v25isuplemento.13117

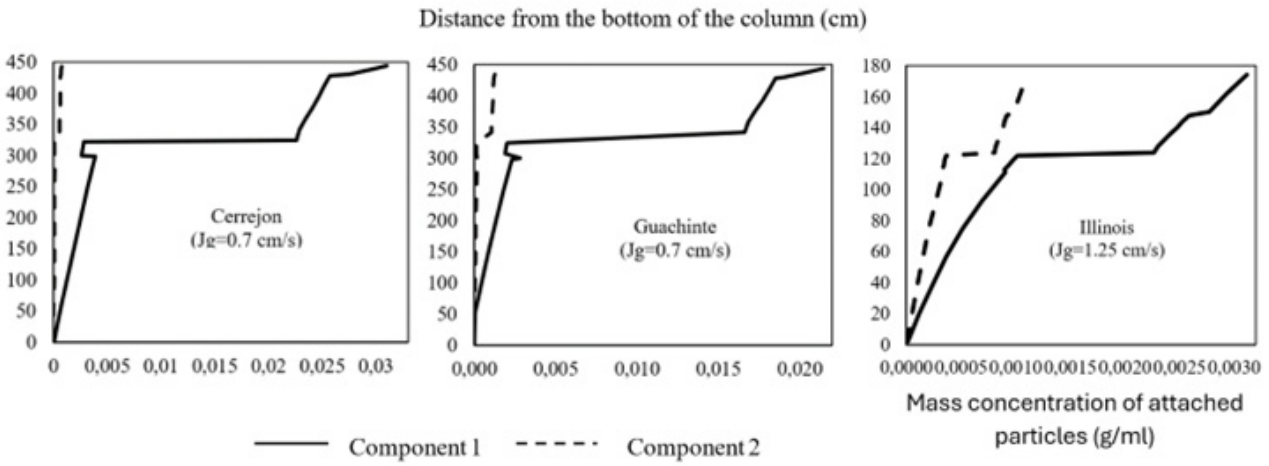

Figure 8. Mass concentrations of attached particles along the flotation column for the organic matter (Component 1) and the mineral matter (Component 2)

The profile of the mass concentration of free particles concerning the height of the column is shown in Figure 9. It is noted, that the concentration of free particles of both components increases along the flotation column. It is observed in Figure 9 that for the Cerrejon and Guachinte coals in the collection zone (feed point, 300 cm) highest values of components 1 and 2 are the achieved; 0.013 gr/ml for component 1 and 0.003 gr/ml for component 2 in the Cerrejon coal, 0.01 gr/ml for component 1 and 0.0056 gr/ml for component 2 in the Guachinte coal.

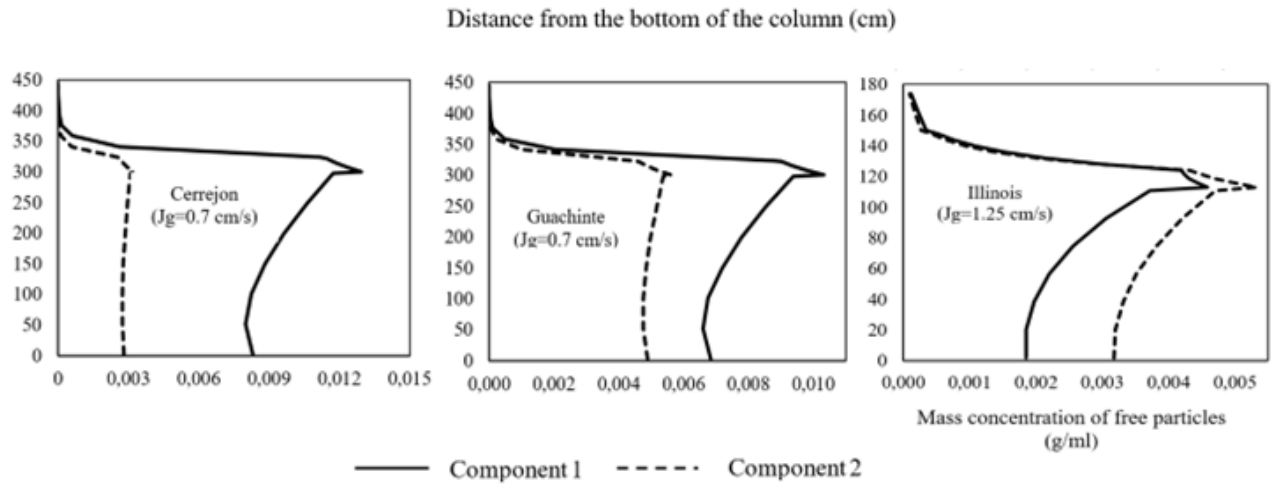

Figure 9. Mass concentrations of free particles along the flotation column for the organic matter (Component 1) and the mineral matter (Component 2)

doi: 10.25100/iyc.v25isuplemento.13117

For Illinois coal in the collection zone (feed point, 113 cm), an opposite effect is observed, the maximum value obtained for component 2 was 0.0052 gr/ml, and for component 1 the value obtained was of 0.004 gr/ml, those difference might be due to the air velocity, where the Illinois coal (simulation 3) presents a higher value (1.25 cm/s) in comparison with the Cerrejon and Guachinte coals (0.7 cm/s, simulations 1 and 2). Component 1 reaches high concentrations, which are in, concordance with the particle mass flow rate (concentration) entering the feed stream. It is noteworthy that after passing through the feeding zone, the concentration profile of both components decreases to values as small as: $6.81x10^{-6}$, $3x10^{-6}$ gr/ml (at approximately 400 cm of length), and $8.9x10^{-5}$ gr/ml (at approximately 174 cm in length) for the Cerrejon, Guachinte, and Illinois coals respectively, which is related, with the entry of free particles into the froth zone of the flotation column, which drops back to the collection zone as a consequence of washing water flow rate (13). These results indicate that the proposed mathematical model shows a good selectivity between the organic and mineral matter of coal.

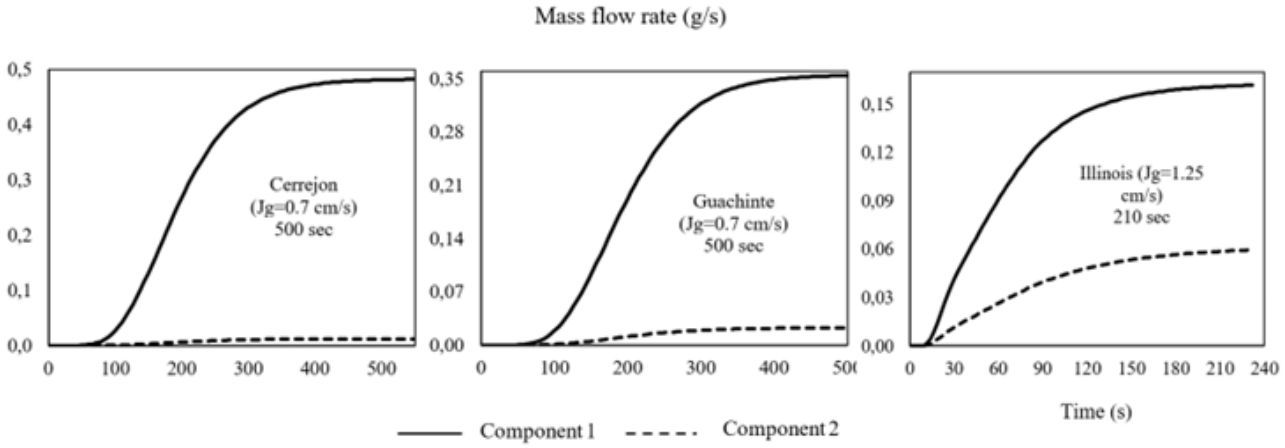

Figure 10. Mass flow rates at the top of the flotation column for the organic matter (Component 1) and the mineral matter (Component 2)

Figure 10 shows the organic matter and mineral matter mass flow rate of the three coal samples obtained at the top of the flotation column as a function of time. The behavior of both flow rates is upward, achieving stability approximately at 500 seconds for the Cerrejon and Guachinte coals and 210 seconds for the Illinois coal. From Figure 8 might be seen that the highest value of the organic matter mass flow rate is obtained by the Cerrejon coal (0.48 gr/s) followed by the Guachinte coal (0.35 gr/s) and the Illinois coal (0.16 gr/s). Regarding the mineral matter mass flow rate shows an opposite effect, Cerrejon coal has the lowest value (0.01 gr/s), Illinois coal has the highest value (0.06 gr/s), and Guachinte coal has a value intermediate (0.02 gr/s). These values show that the mineral matter content is low compared to the organic matter content at the top of the flotation column, indicating the excellent selectivity offered by the proposed mathematical model.

Model validation: to validate the proposed mathematical model, was used the experimental results were obtained with three samples of coal in a flotation column. Figure 11 shows the comparison between the experimental and simulated data for Jg values: 0.7, 1.4, and 2.4 cm/s for the Cerrejon and Guachinte coals, and for the Illinois coal the Jg values were 1.25, 1.50, 1.75, 2.0 and 2.25 cm/s, tailing flow rate remained constant.

doi: 10.25100/iyc.v25isuplemento.13117

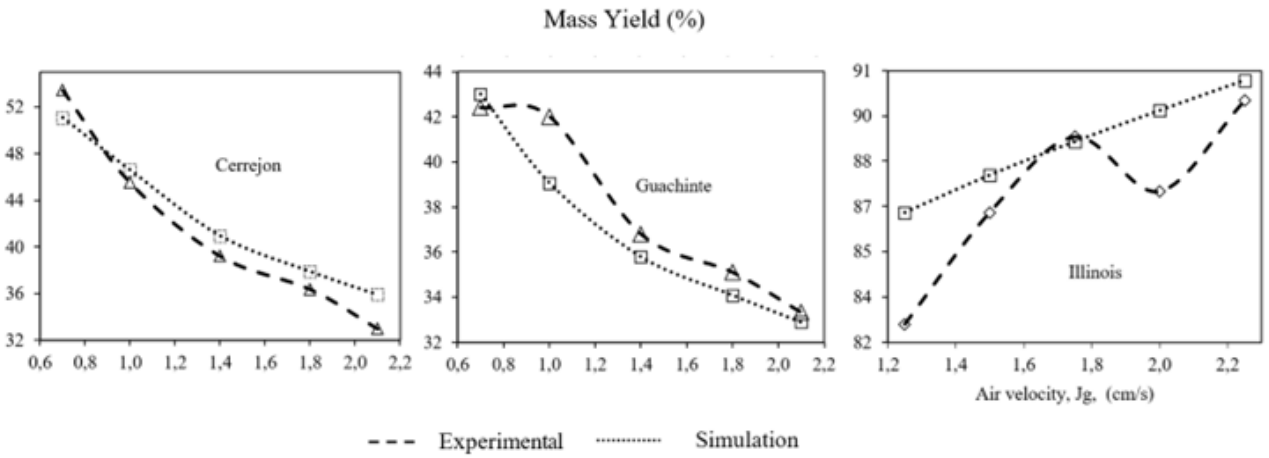

Figure 11. Mass yield vs air velocity (Jg)

The simulated response presents a similar tendency to the experimental response for the Cerrejon and Guachinte coals with the increase in the air velocity, the mass yield decreases for the Illinois coal, and an opposite effect occurs, with the increase in the air velocity, the mass yield increases. For the three coal samples, the percentage error between the experimental and simulated results was; 4.9, 2.4, and 2.0 % for the Cerrejon, Guachinte, and Illinois coals respectively, showing excellent results and estimates of the proposed mathematical model and the established assumptions.

Conclusions

The result of the different simulations established that the proposed mathematical model allows for obtaining good predictions of the dynamic behavior in a flotation column, showing low error percentages. The mathematical model predictions were compared with experimental results obtained in a test-rig flotation column and showed to fit reasonably between the experimental and simulated responses.

The mathematical model development includes the effects of bubble load, slurry density, and viscosity. The equations that represent the collection and froth zone adequately describe the flow regime, the air holdup at the interface, and the transport of solid species. A relevant characteristic is that mathematical model equations might be solved for different ranges of operation conditions. On the other hand, the model does not require the estimation of a large number of parameters. The equations are based on operating conditions such as feed and air flow rate, bubble size distribution, solids size distribution, and column geometry.

It is important to highlight that the proposed model mathematical can describe the dynamic behavior of both phases (air phase-solid phase) throughout all the different column zones of the flotation column. Similarly, it shows a description of the interactions between air bubbles and the particles. On the other hand, does not require the estimation of a large number of parameters.

The particle concentration profile along the flotation column shows a great reduction in the free solids concentration at the top of the froth zone and a decrease in the concentration of attachment solids due to the reductions in the available bubble's surface area. In general, the solids concentration decreases with the height froth while the solids concentration increases with

doi: 10.25100/iyc.v25isuplemento.13117

height along the collection zone, which is similar to other works on the behavior of a flotation column (26).

Acknowledgments

The authors would like to acknowledge the support of the Universidad del Atlántico through the Project: Caribbean impact; "Production of activated coals to remove heavy metals starting at coal mining waste benefited by flotation processes", ING03.CIC2014, financial support.

Referencias Bibliográficas

(1) Piñeres, J., Barraza, J. Effect of pH, air velocity and frother concentration on combustible recovery, ash and sulphur rejection using column flotation. Fuel Processing Technology, 2012, (97), 30-37. https://doi.org/10.1016/j.fuproc.2012.01.004
(2) Piñeres , J., Barraza , J., Bellich, S. Effect of diesel oil and mixture of alcohol-glycol ether on Colombian ultrafine coal leaning using a test-rig loop flotation column. Ingeniería e investigación 2022, (42), (e88273).https://doi.org/10.15446/ing.investig.v42n1.88273
(3) Carvalho, T., Durão, F., Fernandes, C. Dynamic characterization of column flotation process: Laboratory case study. Minerals Engineering, 1999, (12), 1339-1346. https://doi.org/10.1016/S0892-6875(99)00121-1
(4) Cruz, E. A comprehensive dynamic model of the column flotation unit operation. Ph.D. Thesis, 1997, Department of mining and minerals engineering, Virginia Polytechnique Institute and State University, Blacksburg, Virginia. A Comprehensive Dynamic Model of the Column Flotation Unit Operation (vt.edu)
(5) Bouchard, J., Desbiens, A., Del Villar, R., Nunez., E. Column flotation simulation and control: An overview. Minerals Engineering, 2009, (22), 519-529.https://doi.org/10.1016/j.mineng.2009.02.004
(6) Bouchard, J., Desbiens, A., del Villar, R. Column flotation simulation: A dynamic framework. *Minerals Engineering*, 2014, (55) 30–41. http://dx.doi.org/10.1016/j.mineng.2013.07.021
(7) Yahui, T., Maryam, A., Xiaoli, L., Fei, L., Stevan, D. Three-Phases Dynamic Modelling of Column Flotation Process. IFAC (International Federation of Automatic Control) PapersOnLine; 2018, (51), 99-104. https://doi.org/10.1016/j.ifacol.2018.09.399
(8) Yianatos, J., Vallejos, P., Graub, R., Yañez, A. (2020). New approach for flotation process modelling and simulation, 2020, (156), 106482. https://doi.org/10.1016/j.mineng.2020.106482
(9) Himmelblau, D., Bischoff, B. Process analysis and simulation. Chapter 4. 1968, John Wiley & Sons, New York.
(10) Walas S, Modeling with differential equations in Chemical Engineering. 1991, Butterworth-Heinemann, Printed in the United State of America.
(11)Dobby G., Finch J. Particle collection in columns, gas rate and bubble size effects. Canadian Metallurgical Quarterly, 1986, (25), 9-13. https://doi.org/10.1179/cmq.1986.25.1.9
(12) Dobby, G., Finch, J. Flotation column scale-up and modelling. CIM Bulletin, 1986, (79), 89-96. https://store.cim.org/en/flotation-column-scale-up-and-modelling
(13) Finch, J. & Dobby, G. Column Flotation. 1990, Pergamon Press.
(14) Patwardhan, A., Honaker, R. Development of a carrying-capacity model for column froth flotation. International Journal of Mineral Processing, 2000, (57), 275-293. https://doi.org/10.1016/S0301-7516(99)00081-2
(15) Calvo, M., Grecco, A. Predicción del comportamiento dinámico de una columna de flotación a través de un modelo matemático, 2015, [Undergraduate thesis, Universidad del Atlántico, Barranquilla, Colombia]. http://biblioteca.uniatlantico.edu.co
(16) Yianatos, J., Finch, J., Dobby, G., Manqui X. Bubble size estimation in bubble swarm. Journal of Colloid and Interface Science, 1988, (126), 37 – 44. https://doi.org/10.1016/0021-9797(88)90096-3

doi: 10.25100/iyc.v25isuplemento.13117

(17) Thomas, D. Transport characteristics of suspension: VIII. A note on the viscosity of Newtonian suspensions of uniform spherical particles. Journal of colloid and interface science, 1965, (20) 267 277. https://doi.org/10.1016/0095-8522(65)90016-4
(18) Richardson, J., Zaki, W. The sedimentation of a suspension of uniform spheres under conditions of viscous flow. Chemical Engineering Science, 1954, (3), 65-73. https://doi.org/10.1016/0009-2509(54)85015-9
(19) Luttrell, G., Yoon, R. A flotation column simulator based on hydrodynamic principles. International Journal of Mineral Processing, 1991, (33), 355-368. https://doi.org/10.1016/0301-7516(91)90063-O
(20) Masliyah, J. Hindered settling in a multi-species particle system. Chemical Engineering Science, 1979, (34), 1166-1168.https://doi.org/10.1016/0009-2509(79)85026-5
(21) Subrahmanyam, T., Forssberg, E. Froth stability, particle entrainment and drainage in flotation - A review. International Journal of Mineral Processing, 1988, (23), 33-53. https://doi.org/10.1016/0301-7516(88)90004-X
(22) Ata, S. Phenomena in the froth phase of flotation — A review. International Journal of Mineral Processing, 2012 (103), 1–12.
https://doi.org/10.1016/j.minpro.2011.09.008
(23) Tao, D., Li, B., Jhonson S., Parehk, B. A flotation study of refuse pond coal slurry. Fuel Processing Technology, 2002, (76), 201 – 210.https://doi.org/10.1016/S0378-3820(02)00025-5
(24) Piñeres, J., Barraza, J. Energy barrier of aggregates coal particle–bubble through the extended DLVO theory, International Journal of Mineral Processing, 2011, (100), 14–20. https://doi.org/10.1016/j.minpro.2011.04.007
(25) Honaker, R., Monhanty, M., Crelling J. Coal maceral separation using column flotation. Mineral Engineering, 1996, (9), 449–464.
https://doi.org/10.1016/0892-6875(96)00030-1
(26) Falutsu, M., Dobby, G. Froth Performance in Commercial-Sized Flotation Columns. Minerals Engineering, 1992, (5), 1207-1223.
https://doi.org/10.1016/0892-6875(92)90160-B

doi: 10.25100/iyc.v25isuplemento.13117